

Single-Cell Profiling Reveals Functional Heterogeneity and Serial Killing in Human Peripheral and Ex Vivo-Generated CD34+ Progenitor-Derived Natural Killer Cells

Citation for published version (APA):

Subedi, N., Verhagen, L. P., de Jonge, P., Van Eindhoven, L. C., van Turnhout, M. C., Koomen, V., Baudry, J., Eyer, K., Dolstra, H., & Tel, J. (2023). Single-Cell Profiling Reveals Functional Heterogeneity and Serial Killing in Human Peripheral and Ex Vivo-Generated CD34+ Progenitor-Derived Natural Killer Cells. *Advanced Biology*, 7(4), Article 2200207. <https://doi.org/10.1002/adbi.202200207>

DOI:

[10.1002/adbi.202200207](https://doi.org/10.1002/adbi.202200207)

Document status and date:

Published: 01/04/2023

Document Version:

Publisher's PDF, also known as Version of Record (includes final page, issue and volume numbers)

Please check the document version of this publication:

- A submitted manuscript is the version of the article upon submission and before peer-review. There can be important differences between the submitted version and the official published version of record. People interested in the research are advised to contact the author for the final version of the publication, or visit the DOI to the publisher's website.
- The final author version and the galley proof are versions of the publication after peer review.
- The final published version features the final layout of the paper including the volume, issue and page numbers.

[Link to publication](#)

General rights

Copyright and moral rights for the publications made accessible in the public portal are retained by the authors and/or other copyright owners and it is a condition of accessing publications that users recognise and abide by the legal requirements associated with these rights.

- Users may download and print one copy of any publication from the public portal for the purpose of private study or research.
- You may not further distribute the material or use it for any profit-making activity or commercial gain
- You may freely distribute the URL identifying the publication in the public portal.

If the publication is distributed under the terms of Article 25fa of the Dutch Copyright Act, indicated by the "Taverne" license above, please follow below link for the End User Agreement:

www.tue.nl/taverne

Take down policy

If you believe that this document breaches copyright please contact us at:

openaccess@tue.nl

providing details and we will investigate your claim.

Single-Cell Profiling Reveals Functional Heterogeneity and Serial Killing in Human Peripheral and Ex Vivo-Generated CD34+ Progenitor-Derived Natural Killer Cells

Nikita Subedi, Liesbeth Petronella Verhagen, Paul deJonge, Laura C. Van Eyndhoven, Mark C. van Turnhout, Vera Koomen, Jean Baudry, Klaus Eyer, Harry Dolstra, and Jurjen Tel*

Increasing evidence suggests that natural killer (NK) cells are composed of distinct functional subsets. This multifunctional role has made them an attractive choice for anticancer immunotherapy. A functional NK cell repertoire is generated through cellular education, resulting in a heterogeneous NK cell population with distinct capabilities responding to different stimuli. The application of a high-throughput droplet-based microfluidic platform allows monitoring of NK cell-target cell interactions at the single-cell level and in real-time. A variable response of single NK cells toward different target cells is observed, and a distinct population of NK cells (serial killers) capable of inducing multiple target lysis is identified. By assessing the cytotoxic dynamics, it is shown that single umbilical cord blood-derived CD34+ hematopoietic progenitor (HPC)-NK cells display superior antitumor cytotoxicity. With an integrated analysis of cytotoxicity and cytokine secretion, it is shown that target cell interactions augment cytotoxic as well as secretory behavior of NK cells. By providing an integrated assessment of NK cell functions by microfluidics, this study paves the way to further functionally characterize NK cells ultimately aimed to improve cancer immunotherapy.

1. Introduction

Natural killer (NK) cells are a subgroup of type 1 innate lymphoid cells capable of inducing cytolytic activity against virus-infected


or cancer cells. Unlike other lymphocytes, these cells do not need prior antigen sensitization and induce rapid lysis of target cells upon identification without harming healthy tissue.^[1] Apart from cytotoxicity, NK cells also secrete immune-stimulating molecules that modulate the functions of other immune cells.^[2] This functional versatility has enhanced the popularity of NK cells for anticancer immunotherapy.^[3] The allogenic infusion of NK cells derived from different sources has now become a popular mode of NK cell-based therapy with positive clinical outcome in hematological malignancies.^[4,5]

Although NK cell immunotherapy has made progress over the past decade, a better understanding of NK cell biology and heterogeneity will provide knowledge to improve current therapies and develop future treatment strategies. The high degree of heterogeneity within the NK cell population have been shown to impact the overall efficacy of NK cell-based anti-

cancer therapy.^[6-9] Advancing single cell-based technologies have allowed detailed monitoring of individual cells associating the variations within effector functions in NK cells as one of the potential reasons for lower clinical impact of NK cell-based

N. Subedi, L. P. Verhagen, L. C. Van Eyndhoven, V. Koomen, J. Tel
Laboratory of Immunoengineering
Department of Biomedical Engineering
Eindhoven University of Technology
Groene Loper 5, Eindhoven 5600 MB, The Netherlands

N. Subedi, L. P. Verhagen, L. C. Van Eyndhoven, J. Tel
Institute for Complex Molecular Systems
Eindhoven University of Technology
Groene Loper 5, Eindhoven 5600 MB, The Netherlands
E-mail: j.tel@tue.nl

 The ORCID identification number(s) for the author(s) of this article can be found under <https://doi.org/10.1002/adbi.202200207>.

© 2022 The Authors. Advanced Biology published by Wiley-VCH GmbH. This is an open access article under the terms of the Creative Commons Attribution-NonCommercial License, which permits use, distribution and reproduction in any medium, provided the original work is properly cited and is not used for commercial purposes.

DOI: 10.1002/adbi.202200207

P. Jonge, H. Dolstra
Department of Laboratory Medicine – Laboratory of Hematology
Radboud Institute of Molecular Life Sciences
Radboud University Medical Center
Nijmegen 6525 GA, The Netherlands

M. C. Turnhout
Soft Tissue Engineering and Mechanobiology
Department of Biomedical Engineering
Eindhoven University of Technology
Groene Loper 5, Eindhoven 5600 MB, The Netherlands

J. Baudry, K. Eyer
Laboratoire Colloïdes et Matériaux Divisés (LCMD)
ESPCI Paris
PSL Research University
CNRS UMR8231 Chimie Biologie Innovation, Paris 75005, France

K. Eyer
Laboratory for Functional Immune Repertoire Analysis
Institute of Pharmaceutical Sciences
D-CHAB, ETH, Zürich, Zurich 8093, Switzerland

immunotherapies.^[10] Additionally, mass cytometry-based data demonstrated that the overall function of NK cells results from the combined efforts of multiple diverse individual cells.^[11] Recent single-cell RNA sequencing-based studies identified specific markers within NK cell transcriptomes that could eventually be clustered into different functional subpopulations.^[6,8,12,13] Furthermore, using a microwell-based single-cell platform, Vanherberghen and co-workers identified rare serial killer NK cells with superior cytotoxic behavior which accounted for more than 50% of total lysis.^[1] Hence, single-cell-based tools lay the basis for a new era in dissecting heterogeneity within the immune cells to address the functional ability of individual cells.^[14,15]

Innovation in microsystems and microfluidics facilitated the integration of numerous complex functions on-chip to dynamically monitor immune cell activities in real time.^[16] However, the challenge of adopting microsystems/microfluidics technology with such interaction-based immunoassays still remains efficient cell pairing together with the high throughput ability of the systems.^[17] The studies involving highly dynamic cells, such as NK cells, require efficient screening tools that could accurately identify potent cytotoxic cells among the heterogeneous population and allow their characterization.^[10] To meet these requirements, we have presented a high throughput droplet-based microfluidics platform to provide a combinatorial assessment of cytotoxicity and secretory functions within the NK cell population. Here, we monitored around 80 000 droplets over 10 h in real-time to probe the phenotypical and functional heterogeneity of single human Peripheral Blood (PB)-NK cells and ex vivo-generated UCB-derived CD34⁺ HPCs NK cells. Furthermore, we observed a subpopulation within these NK cell sources with superior serial killing ability. By pairing NK cells with distinct target cells, we demonstrated that NK cell-mediated cytotoxicity and cytokine secretion are dynamic processes restricted to a percentage of single NK cells equipped with this ability. In this way, we provide an integrated analysis that paves the way towards phenotypical and functional characterization of NK cells (PB and HPC-NK cells) for channeling new avenues in NK cell-based cancer immunotherapy.

2. Results

2.1. Single-NK Cell Activation in Droplets Using K562 and IL2

To study the diversity within the NK cell compartment, we utilized droplets-based microfluidics for single NK cells activation with K562 cells and cytokines in an isolated environment with reduced paracrine interaction within cells. NK cells were labeled with cytokine catch reagents for IFN- γ and TNF- α to allow for capturing and monitoring cytokine secretion by single cells.^[18,19] After 4 h of activation, cells were retrieved from the droplets by breaking the emulsion with 1H,1H,2H,2H-Perfluoro-1-octanol (PFO) and prepared for downstream flowcytometric analysis (Figure 1A). Similar to our previous studies with other cell types, the viability of NK cells after culturing in droplets was preserved (Figure S1B, Supporting Information). We used pipette tips for loading cells in microfluidic chips to increase the probability of cellular encapsulation and to achieve optimal cell pairing at a ratio of 1:1 in the oil-water droplets (≈ 70 pL).^[20] The cell loading concentrations were adjusted such

that NK cells were optimally paired with K562 cells, and the percentage of activated cells reflected the cellular interaction. With optimal loading conditions, 65% of the cell-containing droplets showed NK and K562 cell pairing (Figure 1B–D). In summary, our platform allowed us to probe NK cell activation at the single-cell level and their interaction with the target cells.

2.2. Functional Variations Among Different PB-NK Cell Phenotypes at Single-Cell Level

Natural killer cells have been categorized into different functional subgroups based on their expression level of CD56 and CD16 surface markers: 1) Regulatory NK cells (CD56⁺CD16⁻), 2) Cytotoxic NK cells (CD56⁺CD16⁺), and 3) Precytotoxic NK cells (CD56⁺CD16^{+/-}, Figure 2A). With our platform, we assessed the distribution of these subsets in freshly isolated peripheral blood NK cells in both, bulk culture, and single-cell levels with or without the addition of external stimuli. The composition within the population mainly consisted of cytotoxic subgroups of NK cells, $\sim 90\%$ CD56⁺ phenotypes (Figure 2B) mostly when activated together with K562 cells. Even though we hardly observed the regulatory NK cell phenotype in peripheral blood (roughly 3%), activation with IL2 induced a twofold increase in these phenotypes (Figure 2B; and Figure S2A, Supporting Information).

Next, we studied different functions of PB-NK cells at the single-cell level to associate them with the respective phenotypes. IFN- γ and TNF- α secretion were included as functional markers for immune regulation, and CD107a (degranulation marker) as a measure for cytotoxicity.^[21–23] No difference was observed in CD107a expression upon stimulation with the cytotoxic phenotypes while the precytotoxic phenotype dominated the CD107a expression, thus showing enhanced cytotoxic behavior (Figure 2C; and Figure S2B, Supporting Information). The combined stimulation with IL2 and K562 induced the most secretion of IFN- γ by regulatory phenotypes (Figure 2D; and Figure S2C, Supporting Information). Notably, precytotoxic phenotypes were also observed to secrete intermediate levels of IFN- γ compared to cytotoxic phenotypes. All the subgroups showed positive TNF- α secretion when stimulated with IL2 (Figure 2E). Furthermore, the precytotoxic phenotype also formed a major component of the PB-NK cell compartment and expressed intermediate levels of NKp46, generally expressed in mature NK cells (Figure S3A, Supporting Information). These findings strengthen the notion that this subset could be the precursor of the cytotoxic population. As expected, the regulatory phenotypes showed higher expression of NKG2A, while NKp46 was highly upregulated by a more mature regulatory and cytotoxic phenotype (Figure S3A,B, Supporting Information). Collectively, we showed variation among different PB-NK cell phenotypes upon stimulation at single-cell level indicative of heterogeneity within the NK cell compartment.

2.3. NK Cell-Mediated Cytotoxicity is a Dynamic Process and Highly Dependent upon Target Cell Interaction

The interaction dynamics of single NK cells with different target cell types were closely monitored to improve the understanding

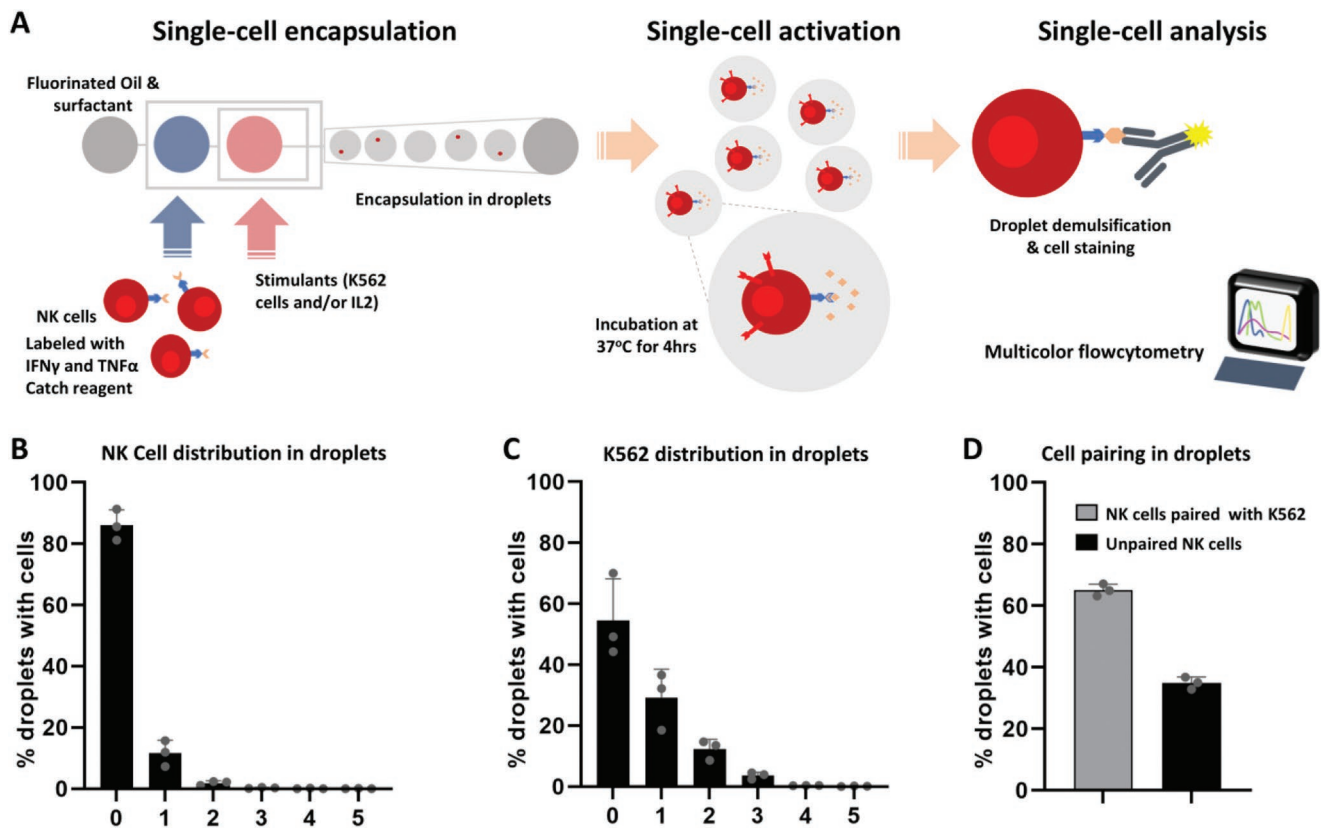


Figure 1. Experimental schematics showing NK cell activation and cytokine secretion assay in droplet: A) Freshly isolated human peripheral blood NK cells were labeled with IFN- γ and TNF- α catch reagent and encapsulated together with stimulants (K562/IL2) into oil/water droplets using a 3-inlet flow-focusing droplet chip with 25 μ m height. After 4 h, the droplets were dissolved using PFO solution to retrieve the cells, which were thereafter labeled for FACS analysis. B) The distribution of cellular encapsulation of NK cells C) or K562 cells in the droplets. D) Cell pairing distribution in droplets. Results are shown as the mean \pm SEM of $n = 3$ independent experiments with different donors.

of cytolytic function. Previously, we developed a droplet-based single-cell platform for high throughput and real-time analysis of cellular cytotoxicity.^[24] We used this platform to monitor over 80,000 droplets per experiment which approximately contained 3,500 droplets with a 1:1 NK cell: target cell ratio (Figure 3A). Individual droplets were monitored for 10 h and subsequently analyzed with an automated script to identify possible cytotoxic events (Figure 3B). During incubation, we observed around 3% target cell division (data not shown), however, all the E:T ratios were defined based on observation at $t = 0$.

PB-NK cells showed a significant variation in the cytolytic function upon interaction with different target cells (Figure 3C). Where single PB-NK cells lysed around 25% (± 2.25 ; $n = 3$) of K562 cells, only 10% (± 4.318 ; $n = 3$) of THP-1 and 8% (± 0.271 ; $n = 3$) of Daudi cells were killed by single PB-NK cells. We observed similar variations using a bulk-based cytotoxicity assay, thereby benchmarking our single-cell findings. For K562 and Daudi cells, most of the cytotoxic events were observed within the first 4 h of cellular interaction, while lysis of THP-1 cells occurred at later time points (Figure 3D). This variation in lytic abilities of PB-NK cells could be linked with the differential expression of the MHC-I molecules expressed by different target cells (Figure S4, Supporting Information).

Zooming in on the killing events revealed that 42% of NK cells (fast killers) induced killing as early as 1 h. In total 69%

of NK cells were able to kill K562 cells during 4 h of interaction (Figure 3E). The remaining 31% of cells (slow killers) only induced cytotoxicity at later time intervals. The observation of these early and late lytic events implies differential regulation in target cell recognition and the involvement of different cytotoxic mechanisms shown by different NK cells with regard to different target cells. Two distinct cytotoxic mechanisms were shown to act on different time scales, with rapid granule-mediated cell death and slower CD95-induced or TRAIL-induced apoptosis.^[25] These striking differences in lytic ability observed between individual NK cells, together with their variation in killing behavior toward different target cells further strengthen the notion toward the existence of heterogeneity within the PB-NK cell population.

2.4. Identification of Rare Serial Killing Events Executed by NK Cells Using the Droplet-Based Single-Cell Platform

There exists a small fraction of NK cells endowed with an immense capacity to kill and handle most of the target cell lysis.^[1,25] These cells, also known as serial killers, can kill over 3 target cells consecutively and are a pursued phenotype for application in cancer immunotherapy. The fraction of serial killer NK cells is however relatively low and other than

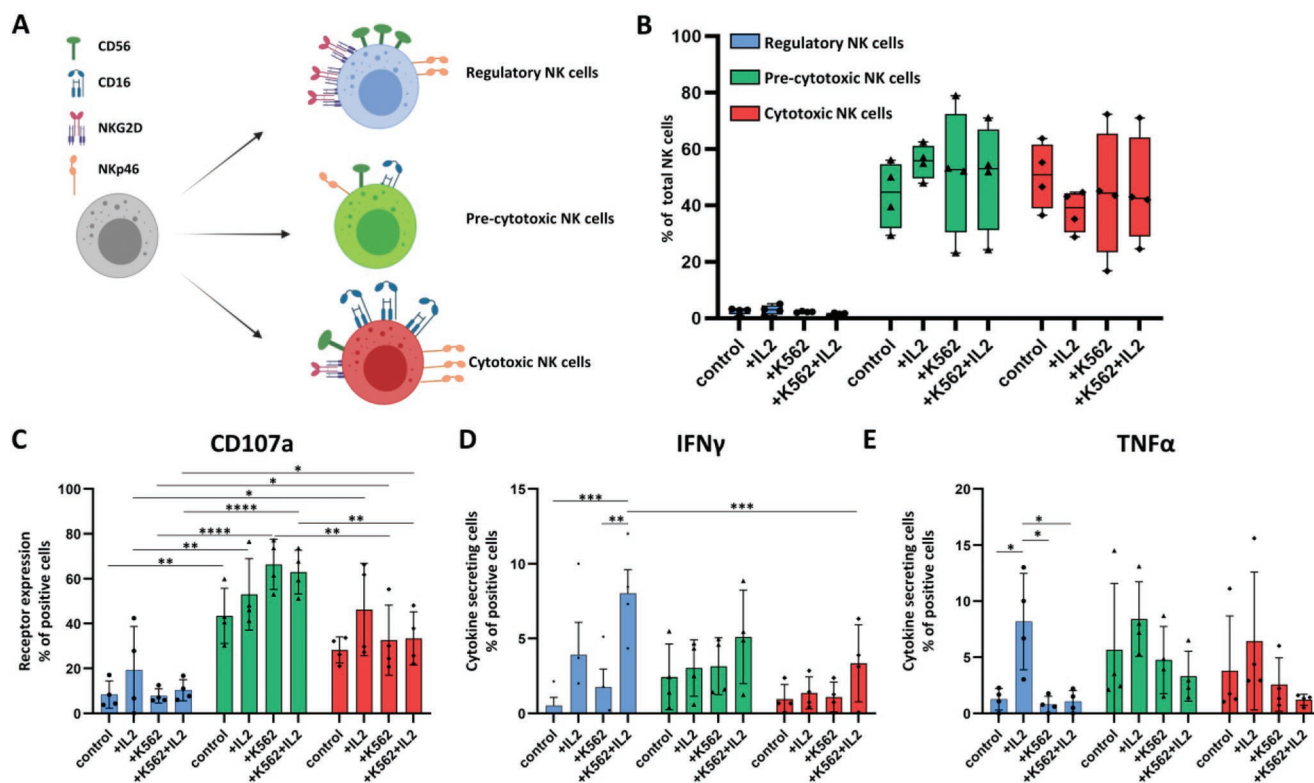


Figure 2. Phenotypical and functional heterogeneity within peripheral blood NK cells: A) Schematics of NK cell heterogeneity with different functional subgroups within the NK cell population. B) Graphs showing distribution of different subgroups of PB-NK cells (regulatory, precytotoxic, and cytotoxic) in droplets. C–E) Graphs showing the percentage of NK cells population positive for: C) CD107a, D) IFN- γ ; E) TNF- α , when stimulated in droplets with IL2, K562, or IL2 and K562 combination. Results are shown as the mean \pm SEM of $n = 4$ independent experiments with different donors; blue, green, and red bars represent regulatory, precytotoxic, and cytotoxic phenotypes, respectively. Statistical significance was determined by two-way ANOVA followed by posthoc Tukey's multiple comparison test; * $p < 0.05$, ** $p < 0.01$, *** $p < 0.001$, **** $p < 0.0001$.

their superior killing ability, not much is yet known about them.

We, therefore, adapted the microfluidic platform by tuning the droplet size and cell loading concentrations and utilized the strength of our approach to study these potent serial killers in high throughput. With larger droplets (1.2 nL volume) we increased the fraction of droplets containing multiple target cells (≥ 3) with single NK cells to around 3% (242 droplets) (Figure 4A,B). Exploring different E:T ratios, i.e., 1:1, 1:2, 2:1, and 3:1, variations in lysis of target cells were distinctly observed (Figure 4C). At a 1:1 ratio, a lower fraction of death in K562 cells was seen in bulk than compared to droplets at a 1:1 ratio. In contrast, at a 1:2 ratio around 50% (± 4.7 ; $n = 4$) of paired K562 cells were killed by single encapsulated NK cells in the droplet and this was higher than observed in bulk-based measurements. When single K562 cells were paired with either 2 or 3 NK cells in droplets, the percentage of cell death increased and was somewhat higher than the corresponding bulk-based assay. By comparing the significantly low killing events with unpaired K562 (in-droplet controls), we ruled out the possibility of spontaneous cell death in the droplets (Figure 4C).

We defined serial killing activity as a single NK cell that could consecutively lyse ≥ 3 target cells within 10 h. Zooming in on droplets with 1 NK cell and 3 or more target cells, we observed 12% (± 0.736 , $n = 3$) serial killing events by PB-NK cells (Figure 4D,E; and Figure S5, Supporting Information).

Additionally, we observed in 49% (± 8.06 , $n = 3$) of droplets with less than 3 K562 cells target cell lysis and 37% (± 9.68 , $n = 3$) droplets showed no target cell lysis. To ensure multiple cell encapsulation, we enhanced the droplet size which however resulted in later cellular interactions between NK and target cell, thus decreasing the percentage of early positive events upon incubation.^[26]

Interestingly, using our droplet-based assay we segregated and created multiple conditions with a high-throughput resolution to investigate the killing properties of NK cells. This enabled us to identify a rare serial killer subset in the PB-NK cell population where single NK cells are capable of lysing over three K562 cells. This is a first and important step to opening the possibility of studying these highly searched-for cell types.

2.5. Single Ex Vivo-Generated HPC-NK Cells Display Superior Antitumor Cytotoxicity

A major hurdle in utilizing allogenic PB-NK cells for therapeutic purposes is that only a small fraction of peripheral blood mononuclear cells comprises NK cells, and thus generating them in sufficient numbers to meet clinical requirements can be challenging.^[27] Recently, other sources for NK cells, such as umbilical cord blood (UCB) have therefore been successfully explored^[28–30] As a major advantage, UCB-derived CD34+

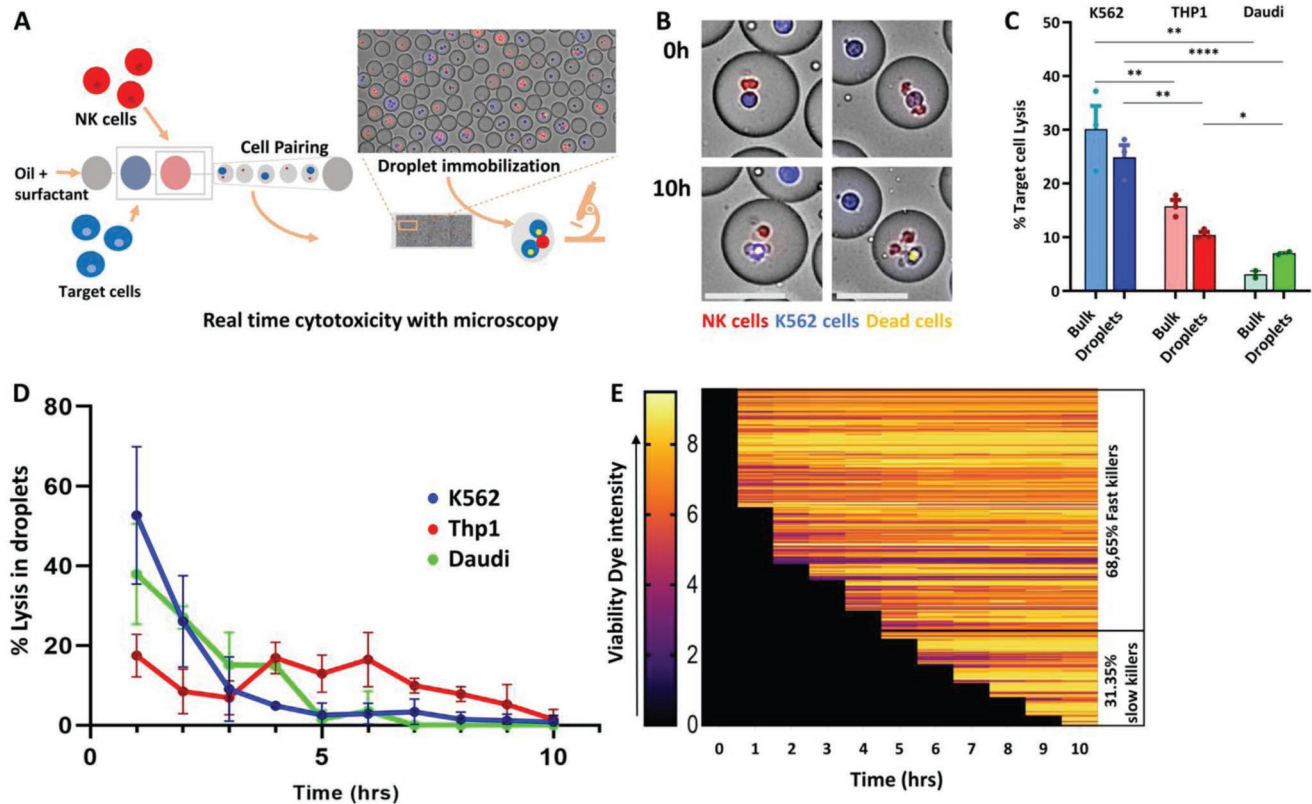


Figure 3. NK cell-mediated cytotoxicity at the single-cell level: A) Schematic representation of single-cell cytotoxicity. PB-NK cells were labeled with Calcein Red AM dye (red cells) and K562 cells with Cell Tracker Blue (blue cells) and paired together in 70 pL droplets in presence of viability dye (Sytox green and Cell event Caspase 3/7; yellow cells). Cells were incubated at 37 °C and 5% CO₂ for 10 h. B) Microscopic overview of NK cell-mediated cytotoxicity in droplets. Over the interval of 10 h, NK cells interacted with target cells inducing cytotoxicity. The dead cells were stained with the viability dye turning yellow. Scale bar = 50 μm. C) Bulk versus droplets cytotoxicity assay with K562 (Blue), THP-1 (Red), and Daudi cells (Green). Light and dark colors represent bulk and drop experiments respectively. D) Graph representing the dynamics of cytotoxic events in droplets for different donors. The dynamics were determined for the killer fraction of NK cells, thus showing the percentage of the fast and slow killer population in NK cells. Blue, green, and red lines represent K562, THP1, and Daudi cells, respectively; data analysis was performed on E:T 1:1; Each time point represents new events per hour. E) Heat Map showing the dynamics of cytotoxicity within an experiment. Each line represents individual cells. The graph does not include the droplets with 0, or 1 cell and droplets with dead cells at $t = 0$ h. Results are shown as the mean \pm SEM of $n = 3$ independent experiments with different donors. Statistical significance was determined by two-way ANOVA followed by posthoc Tukey's multiple comparison test; * $p < 0.05$, ** $p < 0.01$, **** $p < 0.0001$.

hematopoietic progenitor cells (HPCs) are more easily available and have several NK cell progenitors with fewer requirements for HLA matching compared to T cells.^[31] This makes UCB-derived HPCs a flexible and attractive source for NK cells.^[29] Upon expansion, these cells display significantly more cytotoxicity in bulk experiments compared to their blood-derived counterparts.^[32]

Given the potency and high translational efficacy of HPC-NK cells, we next sought to determine their tumoricidal activity at single cell level. We observed an enhanced IFN- γ and TNF- α secretion by HPC-NK cells in droplets when paired together with target cells thus ensuring their activation in droplets (Figure 5A). In total 53% (± 7.75 ; $n = 4$) of total lytic events were observed for these NK cells with an increasing trend of lytic events over the period of 10 h (Figure 5B). HPC-NK cells were able to induce significantly higher lytic ability in comparison to PB-NK cells (Figure 5C). At different E:T ratios, both in bulk and at the single-cell level, there was a significant increase in the percentage of cytotoxic events compared to unpaired target cells (Figure 5D). At 1:1, the cytotoxic event in both bulk (51%;

± 7.4 ; $n = 4$) and at the single-cell level (54%; ± 2.4 ; $n = 4$) was similar, but with other E:T ratios the number of cytotoxic events increased in droplets despite the number of effector or target cells inside. A large fraction of NK cells with serial killing ability was identified in HPC-NK cells compared to PB-NK cells (Figure 5E,F). Of the total droplets with over 3 target cells, we observed around 34% (± 3.2 ; $n = 4$) of HPC-NK cells had lysed over 3 target cells successively. We also observed a higher percentage of droplets with positive cytotoxic events (48%; ± 4.0 ; $n = 4$), while the droplets with no cytotoxic events remained at a minimum. In conclusion, we showed that ex vivo-generated HPC-NK cells are equipped with superior cytotoxic potential both at the population as well as at the single-cell level.

2.6. NK and Target Cell Coencapsulation Augments IFN- γ Secretion

To obtain insight into the distinct functional abilities of NK cells, we designed an in-droplet immunoassay to correlate two

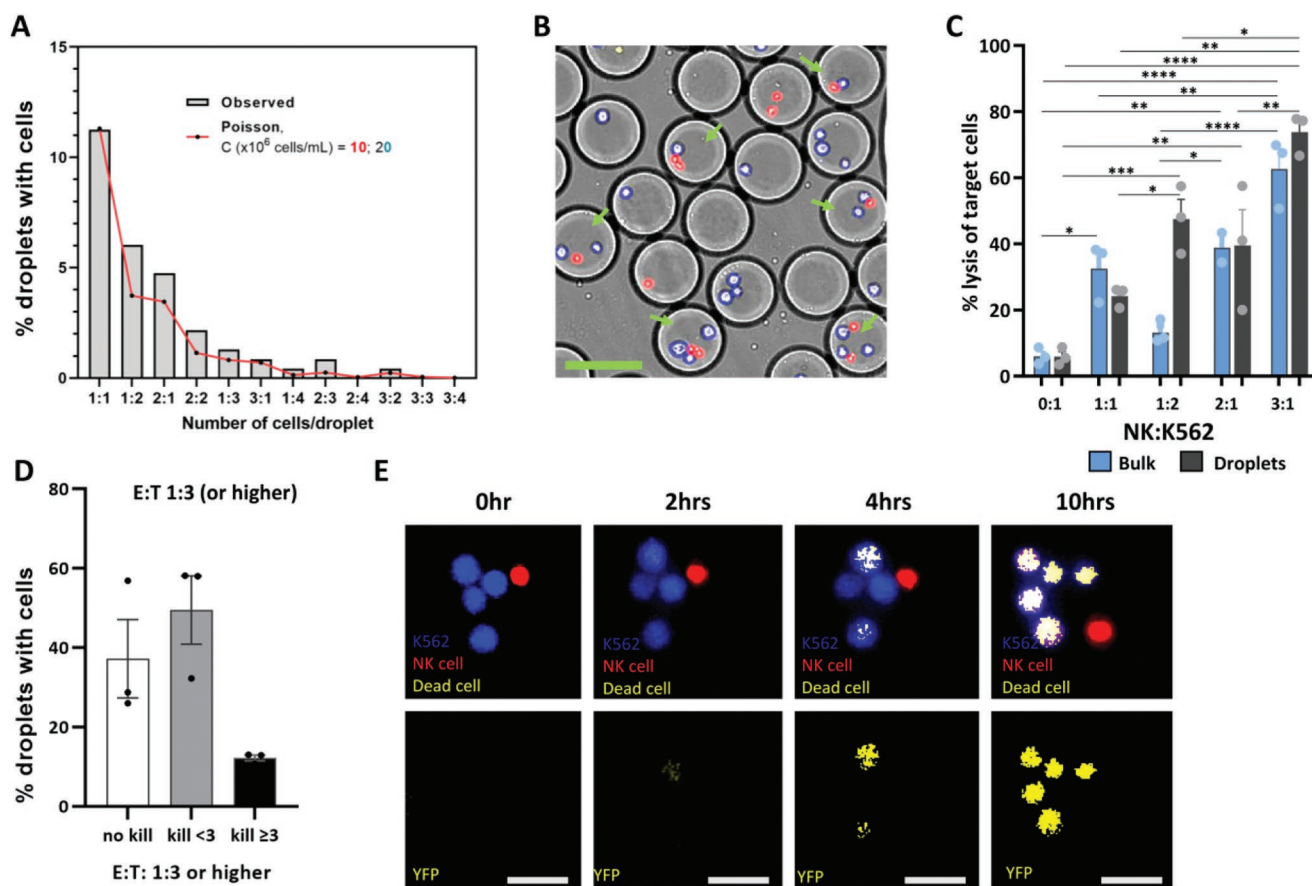


Figure 4. Adaptation of cytotoxicity platform to identify serial killer NK cells: A) Graph showing the experimental (gray bars) and predicted (red line) probability for different cell pairing ratios inside the 1.2 nL droplet. B) Microscopic overview of different E:T ratios for NK cells (red) and K562 (blue) observed inside the droplet. Scale bar = 50 μ m. C) Bulk (blue) versus droplets (black) cytotoxicity assay with K562 (at 0:1; 1:1; 1:2, 2:1, 3:1 E:T ratio, respectively). D) Graph depicting the percentage of alive K562, <3 dead K562 and ≥ 3 dead K562 within the droplets containing more ≥ 3 or more K562 cells. E) Microscopic overview of a serial killing event in droplets over the period of 10 h. red = NK cells; Blue = K562 cells; yellow = dead cells; scale bar = 50 μ m. Results are shown as the mean \pm SEM of $n = 3$ independent experiments with different donors. Statistical significance was determined by two-way ANOVA followed by posthoc Tukey's multiple comparison test; * $p < 0.05$, ** $p < 0.01$, *** $p < 0.001$, **** $p < 0.0001$.

important functions: cytotoxicity and IFN- γ secretion. To the best of our knowledge, we report for the first time on a droplet-based platform that allows monitoring both functions in single primary NK cells simultaneously in real-time. A similar platform was developed by Antona et al. that also studied these functions in droplets, however, their platform was designed for end-point-based analysis and thus cannot address the temporal dynamics of cellular interactions.^[33] We adapted the “In-drop sandwich immunoassay,” as described by Eyer et al.^[34,35] to allow the combinatorial investigation of IFN- γ release and NK cell cytotoxicity in a time-dependent manner. In essence, each droplet functions as a bio-nanoreactor containing NK cells coencapsulated together with target cells, soluble viability dyes, functionalized magnetic nanoparticles (~3000 per 70 pL droplets), and detection antibodies in solution. Within a magnetic field, the nanoparticles form a uniform bead line. Thus, making each droplet a screening chamber in which cytotoxicity and secretion can be investigated together (Figure 6A,B). To validate our approach, we first generated two batches of droplets that both contained the magnetic capture beads and fluorescently labeled IFN- γ detection antibodies and coencapsulated

either 0 nM IFN- γ or 50 nM soluble IFN- γ . During microscopy, we clearly observed a strong positive signal for the droplet batch with soluble IFN- γ (Figure 6C). The detection limit of the assay now is 1 nM and the secretion below the amount could be detected but not accurately quantified (Figure S6A, Supporting Information).

Next, we integrated this technological advancement in our NK cell killing platform which yielded droplets with 7 different possible combinations (Figure 6D; and Figure S6B, Supporting Information). To examine whether target cell-induced secretory and cytolytic functions were associated with individual NK cells, we monitored the secretion dynamics of an NK cell upon pairing with target cells in real-time. Approximately, 33% of droplets were positive when paired with K562, while only 5% of droplets without target cells showed positive IFN- γ secretion (Figure 6E). Among the total number of droplets with E:T pairing, only 22% (± 1.12 ; $n = 2$) showed both cytotoxicity and secretion, 13% (± 2.9 ; $n = 2$) were positive only for cytolysis, and 10% (± 1.6 ; $n = 2$) for secretion only (Figure 6F). To investigate how the dynamics of contact with target cells could regulate cytolysis and secretion in single NK cells, the droplets with

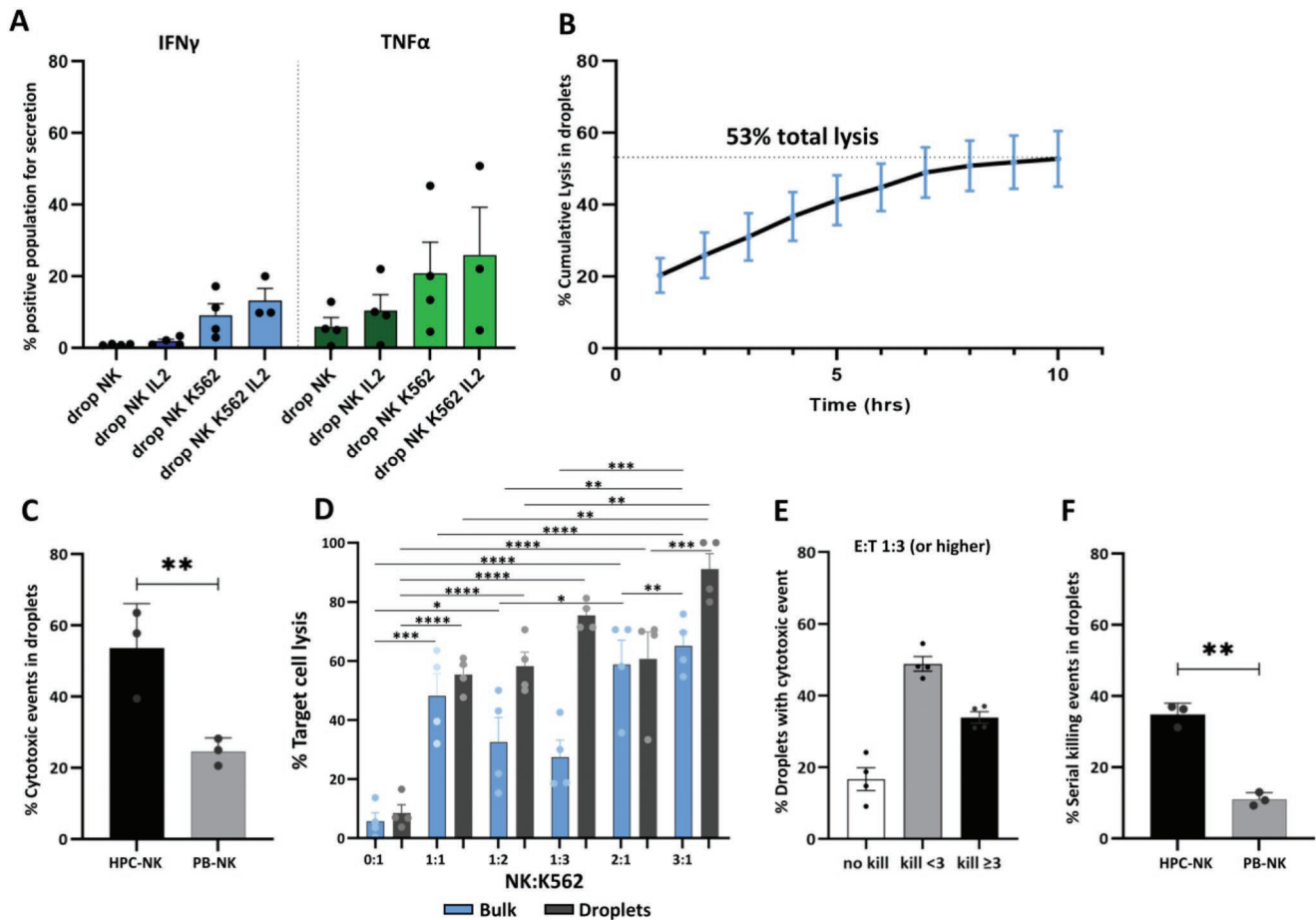


Figure 5. Functional assessment of HPC-NK cells at single-cell level: A) Activation of HPC-NK cells at the single-cell level with different stimulants (IL2, K562, or IL2+K562) to measure the secretion of IFN- γ (Blue bars) and TNF- α (Green Bars). $n = 4$ activation with IL2 and K562; $n = 3$ activation with IL2 and K562. B) Graph representing the dynamics of cumulative cytotoxic events in droplets for different donor-derived HPC-NK cells. The dynamics were determined for the killer fraction of HPC-NK cells; data analysis was performed on all possible E:T. C. Comparison between cytotoxic events between UCB-derived (HPC) NK cells (Black bars) and PB-NK cells (grey bars); $n = 3$. D) Bulk (blue) versus droplets (black) cytotoxicity assay with K562 (at 0:1; 1:1; 1:2; 1:3; 2:1; 3:1 E:T ratio, respectively). E) Graph depicting the percentage of no dead K562, <3 dead K562, and ≥ 3 dead K562 within the droplets containing ≥ 3 K562 cells. F) Comparison between the percentage of serial killers NK cells in HPC-NK cells (UCB-derived; black bars) and PB-NK cells (Gray bars). Results are shown as the mean \pm SEM of $n = 4$ independent experiments with different donors (other than denoted differently). Statistical significance was determined by D) Two-way ANOVA followed by posthoc Tukey's multiple comparison test; $*p < 0.05$, $**p < 0.01$, $***p < 0.001$, $****p < 0.0001$. C&F. Student t -test $**p < 0.01$.

positive events for both cytolysis and secretion were monitored closely. On average, an NK cell would already induce a lytic event within the first 3 h of interaction (data not shown), while the secretion followed at around 4.7 h. The highest fraction of IFN- γ -producing cells ($\approx 67\%$) was observed positive within 3–6 h (Figure 6G). Hence these results suggest that secretion follows the lytic event upon interaction with target cells, however, the underlying mechanistic mode of action needs to be further explored.

3. Discussion

Cellular heterogeneity within the NK cell compartment is well appreciated, however, how functional cellular properties are tied to this phenotypical diversity remains largely understudied. It is important to study single cells in a noise-free environment

to exclude juxtacrine or paracrine interactions to fully comprehend NK cell diversification and their ability to induce different effector functions. Therefore, an optimal experimental approach requires both stimulation and analysis with single-cell resolution. By activating NK cells in picolitre size droplets, we ensured that external noise is reduced, and that observed cellular responses reflect intrinsic behavior.

Using our microfluidic platform, we present the functional assessment of ex vivo-generated HPC-NK cells and compared them with peripheral blood NK cells at single-cell level. We successfully demonstrated that HPC-NK cells, upon expansion with cytokines, are significantly more cytotoxic than individually stimulated primary NK cells isolated from peripheral blood. Furthermore, we showed that HPC-NK cells harbor a larger pool of serial killers which is consistent with the percentage of serial killers in HPC-NK cells identified in a recent study using a microwell-based platform.^[32] Interestingly, for all E:T ratios

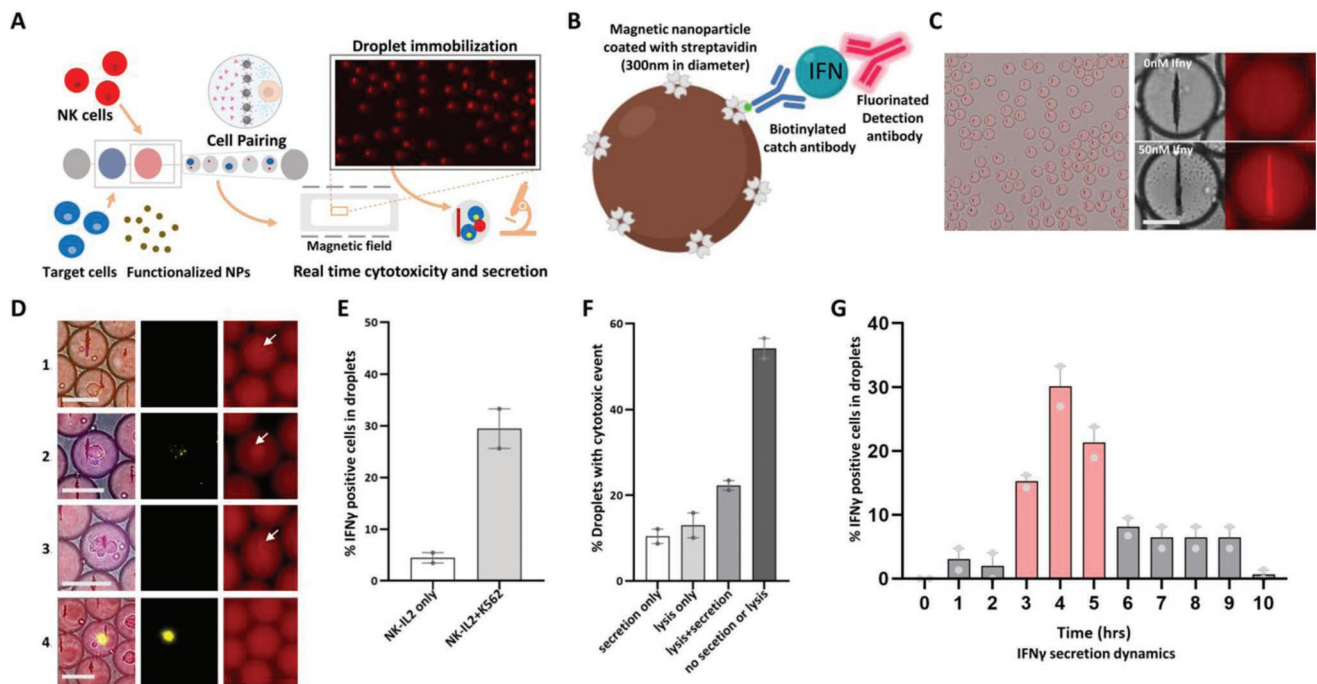


Figure 6. Combinatorial assessment of the cytotoxic and secretory function of PB-NK cells upon target cell interaction: A) Schematics of the in-droplet combinatorial assay. PB-NK cells were labeled with Cell tracker Blue (10 μM) and encapsulated together with target cells and nanoparticles mixed at the concentration of 10 million cells mL^{-1} . A mixture of viability dyes (Sytox green and Cell event caspase3/7 green) was added together with the cells. Oil/water droplets were immobilized in an observation chamber in presence of a magnetic field and monitored for 10 h at 37 $^{\circ}\text{C}$. Each image was captured at an hour interval. B) The magnetic nanoparticle coated with streptavidin allowed binding of biotinylated catch antibody. When secreted IFN- γ binds to the catch antibody, the freely floating detection antibody is relocated into the beads thus forming a fluorescent bead line. C) Microscopic overview of the droplet with fluorescent beadline (left) and zoomed-in view of a droplet with 0 nM IFN- γ (upper right) or with 50 nM IFN- γ (lower right). Scale bar 50 μm . D) Microscopic overview of several conditions analyzed inside droplets; 1) Droplets with only NK cells that secreted IFN- γ ; 2) droplets with NK cells and K562 cells positive for both cytotoxicity and IFN- γ secretion; 3) droplets with NK and K562 and positive only for IFN- γ secretion; 4) droplets with K562 and NK cells positive only for cytotoxicity. Scale bar = 50 μm . E) Graph representing the percentage of NK cells secreting IFN- γ in droplets when incubated only with IL2 (white bars) or with IL2 and K562 (gray bars). F) Graph representing the percentage of droplets with cell pair showing secretion only (white), lysis only (light gray); lysis and secretion (dark gray), and no secretion or lysis (black). G) Dynamics of IFN- γ secretion by NK cells measured over the period of 10 h. Each vertical bar represents independent events per hour. Results are shown as the mean \pm SEM of $n = 2$ independent experiments with different donors.

tested (except for 1:1), we observed a higher percentage of cytotoxicity similar to or higher than bulk-based analysis. These results suggest that the confinement within droplets enhances NK cells' probability of interacting with a target cell compared to a crowded microwell-based setup.^[26] Similar cytotoxic events at different E:T ratios, for example, a similar percentage of lysis with 2:1 and 1:2 (or 3:1 or 1:3) was also observed. This suggests that NK cells within a small group (as inside the droplets), operate independently to mediate the lysis of a single target cell and do not show cumulative cytolytic effect by cooperating with neighboring cells as observed in bulk based cocultures.^[36]

Serial killers have been studied previously for population-based IL-2-activated human PB-NK cells.^[1,37,38] However, it is still not studied how NK cell activation at a single-cell level affects the phenomenon. We identified 12% serial killing events where a single NK cell (upon single-cell activation) could lyse ≥ 3 target cells consecutively. The percentage of serial killers identified in our study is higher than what had been observed in resting NK cells, as shown by Guldevall et al., suggesting that IL2 can enhance the serial killer behavior in NK cells.^[37,39] In line with earlier studies, around 25% of NK cells showed positive cytotoxic events while the remaining other NK cells

did not induce target cell lysis.^[1,24,39] In contrast to the work described by Sarkar et al., we did not observe 100% NK cell-mediated killing in droplets. We believe 100% killing in an earlier study could be due to the characteristics of the utilized dye being actively pumped out by the target cell.^[40]

The FACS-based data from single-cell activation showed an augmented secretory activity of CD56+ phenotypes (both cytotoxic and precytotoxic) upon interaction with their target cells.^[41] We further investigated the correlation between target interaction-induced cytotoxic event and secretory behavior of individual NK cells by incorporating an innovative in-droplet sandwich immunoassay together with our in-droplet cytotoxicity assay. This combinatorial platform provides a unique ability for high throughput monitoring of cytokine secretion in real-time together with cytotoxicity at the single-cell level. To this end, we identified 74% of total lytic events in droplets that showed positive secretory function as well. In this way, we demonstrated a correlation between cytotoxic and secretory function of NK cells, which others were not able to find.^[33,36] We believe that this discrepancy is explained by a short experimental protocol of 4 h leading to a missed cytolytic fraction that also tests positive for IFN- γ .

The dynamics of NK cell-mediated cytotoxicity are dependent on several factors such as the maturation state of NK cells, phenotypical variation based on the expression of several surface molecules, and lytic content of NK cells.^[40] Besides these NK cell-specific factors, the expression of NK-responsive factors in target cells also determines the nature and speed of cell death. In our study, we presented the comparison of NK cell-mediated cytotoxicity with two leukemia (K562 and THP-1) and one lymphoma (Daudi) cell lines, known to show different sensitivity toward NK cells.^[42] Along with the number of cytotoxic events, the differences were also observed in the timeline of the cytotoxicity. This variation could be linked to the surface arrangements of these cells (expression patterns of different activating and inhibitory molecules) which eventually leads to the activation of different killing mechanisms. In agreement with the literature, we observed upregulated expression of HLA molecules by all cell types.^[43–45] NK cells lyse K562 target cells primarily by delivering perforin/granzyme-loaded cytolytic granules into the lytic synapse. However, the lysis of THP-1 cells was more dependent on cytokines, such as IFN- γ which could lead to an increase in ICAM-1 molecule upon exposure.^[46,47] NK cells also kill THP-1 cells by forming nanotubes that generally occur after certain hours of interaction.^[47,48] Involvement of all these different pathways leads to the later killing of THP-1 cells compared to K562.

This study has facilitated studying the functionality of the single-cell immunoassays by incorporating the temporal aspect in the overall assay. The temporal function of the assay suggested that NK cells can kill their target cell in a fast or slow manner. However, this study could not identify the exact mechanism (Perforin-granzyme B based or TRAIL based) involved that could be associated with variation in cytotoxic dynamics. The easiest approach for studying NK cell lytic pathways could be in-droplet proteolytic degradation or drug induced inhibition of perforin to prevent the granzyme-mediated killing or blocking of the TRAIL-Death receptors on the target cells to identify the pathways involved.^[25,49] However, this platform momentarily lacks in terms of further downstream analysis. Droplet sorting with integrated transcriptomic profiling of NK cells with varying killing abilities will provide wider information on the relevance of NK cell heterogeneity ultimately making phenotypic connections with functional characteristics.

Our research emphasizes unraveling the complex functional and phenotypical heterogeneity within the NK cell population. This research provided an integrated analysis of NK-target cell interactions and their implications on the cytolytic and secretory behavior of single NK cells. By adopting the droplet-based cytotoxicity platform, we identified rare serial killers, thus channeling exciting ways for easy identification and characterization of these rare cell types in the future. We believe that our data on functional heterogeneity underlying NK cells, both peripheral NK cells as well as CD34+ HPC-derived NK cells, provides valuable contributions towards developing and elevating the efficacy of NK cell-based cancer immunotherapy.

4. Experimental Section

Cell Isolation and Culture: K562 cells were cultured in a 1:1 v/v mixture of RPMI 1640 (Gibco, Catalog no. 22 400 089) and IMDM (Gibco, Catalog no. 12 440 053) supplemented with 10% fetal bovine serum (FBS;

Gibco) and 1% penicillin/streptomycin (PS; Gibco). THP-1 and Daudi cells were cultured in RPMI, supplemented with 10% FBS and 1% PS. All the cell lines were regularly tested for mycoplasma contamination. PB-NK cells were obtained from buffy coats of healthy donors (Sanquin) after written informed consent according to the Declaration of Helsinki and all experimental protocols concur with institutional guidelines. In short, peripheral blood mononuclear cells (PBMCs) were isolated from donor blood via density gradient centrifugation using Lymphoprep Density Gradient Medium (Stem cell). The NK cells were subsequently isolated using magnet-activated cell sorting (MACS) by negative selection using an NK cell isolation kit (Miltenyi Biotec, Catalog no. 130-092-657) following the manufacturer's instructions. Cells were counted and purity was routinely assessed using flow cytometry by cell surface marker staining for 10 min at 4 °C, using PE-CY7-labeled anti-CD56 (Biolegend, Catalog no. 362 509), PE-labeled anti-CD16 (Biolegend, Catalog no. 302 007), and PerCP-labeled anti CD3 (Biolegend, Catalog no. 300 328) antibodies (50 μ L) FACS buffer (2% FBS in PBS). The NK cells were identified as CD16⁺CD56⁺CD3⁻, and purity was on average 91%. Subsequently, isolated NK cells were encapsulated into droplets with K562 in presence of IL2, as a stimulant (Peprotech, Catalog no. 200-02; 1400 ng mL⁻¹).

HPC-NK Cell Culture and Expansion: Cryopreserved UCB CD34+ progenitor-derived HPC-NK cells from different donors were kindly provided by Dr. Harry Dolstra (Radboudumc, Nijmegen).^[32] The cells were thawed in a medium with 71% Human Serum (HS; Sanquin), 0.03% DNase, and 0.1% MgCl₂ and were washed (at 300 g for 15 min) after 10 min of resting. The cells were then resuspended in NK MACS medium (Miltenyi, Catalog no. 130-107-209) supplemented with 10% HS and 1% NK MACS supplement (Miltenyi) at the concentration of 3 million cells mL⁻¹. The cells suspension (1.5 mL) was loaded into the 6 well plates and supplemented by IL15 (Immunotools, Catalog no. 352 310; 50 ng mL⁻¹) and IL12 (Miltenyi, Catalog no. 130-096-704; 0.2 ng mL⁻¹). On every second day, NK MACS medium (1 mL; with 10%HS, 1% NK MACS Supplement, 50 ng IL15, and 0.2 ng mL⁻¹ IL12) was added to the cells, thus allowing them to expand for 7 days. All the assays were performed after the 6th day of expansion. The culture was kept for 2 weeks after thawing.

Microfluidic Chip for Droplet Production: The three-inlet microfluidic device was developed following the protocols described in Sinha et al.^[20] The microfluidic device was molded using a SU-8 photoresist structure on a silicon wafer and a commercially available polydimethylsiloxane silicone elastomer (Sylgard 184, Dow Corning), mixed with a curing agent at the ratio of 10:1 w/w and allowed to cure for 3 h at 60 °C. The surface of the Sylgard 184 was activated by exposure to plasma and sealed with a plasma-treated glass cover slide to yield closed microchannels. Channels were subsequently treated with a 5% v/v silane (1H,1H,2H,2H-Perfluorooctyltriethoxysilane; Fluorochem, Catalog no. S13150) solution in fluorinated oil (Novec HFE7500, 3 M, Catalog no. 51 243) and thermally bonded for 12 h at 60 °C. The dimensions of the microfluidic channels are 40 \times 30 μ m² at the first inlet, 60 \times 30 μ m² at the second inlet and the production nozzle, and 100 \times 30 μ m² at the collection channel.

Assembly of Droplet Observation Chamber: Glass microscopy slides (76 \times 26 \times 1 mm; Corning) were used as top and bottom covers (76 \times 26 \times 1 mm). Two access holes of 1.5 mm diameter were drilled in the top glass. Both slides were thoroughly cleaned using soap, water, and ethanol, and were exposed to air plasma (60 W) for 5 min. A cutout sheet of 60 μ m thick double-sided tape (ORAFOL) was carefully placed above the bottom glass slide. Afterward, the glass slides were stacked on top of each other, and the assembly was pressed using Atlas Manual 15T Hydraulic Press (Specac) for 5 min at 155 °C at 400 kg m⁻² pressure load. Next, two nano ports (Idex) were attached to the holes using UV curable glue (Loctite 3221 Henkel) which was cured under UV light for 5 min. Subsequently, the surface of the 2D chamber was treated with a 5% v/v silane solution. Finally, the chamber was dried, filled, with fluorinated oil, and sealed until use. The chamber was reused multiple times and cleaned after each experiment by flushing fluorinated oil to remove droplets and was stored until the next use.

Cell Loading in a Microfluidic Chip: Droplets were produced with a three-inlet microfluidic device. The protocol for loading cells in the microfluidic chips is described in Subedi et al.^[24] The droplets of $\approx 50 \mu\text{m}$ diameter were generated using flow speeds of $30 \mu\text{L min}^{-1}$ for oil and $5 \mu\text{L min}^{-1}$ for each sample inlet. For serial killer experiments, droplets of $\approx 130 \mu\text{m}$ diameter were produced using flow speeds of $20 \mu\text{L min}^{-1}$ for oil and $5 \mu\text{L min}^{-1}$ for each sample inlet. The droplets were produced for around 5–10 min, thus generating 700 000 droplets in total. For the stability of droplets, 2.5% v/v Pico-Surf surfactant (Sphere Fluidics, Catalog no. C024) was used in fluorinated oil.

Bulk Activation Assay: NK cells were incubated at 1 million cells per 100 μL in PBA containing IFN- γ Catch Reagent (Miltenyi, Catalog no. 130-090-443) and TNF- α Catch Reagent (Miltenyi, Catalog no. 130-091-268) at 4 °C for 20 min. Next, cells were washed and resuspended in RPMI cell culture medium supplemented with 2% HS, and 1% PS, at 25 000 cells per 100 μL in U-bottom microwell plates together with stimulants (K562 cells at E:T 1:1 or IL2 50 ng mL^{-1} or K562+IL2 at above-mentioned concentrations). The cells were incubated at 5% CO_2 and 37 °C temperature for 4 h.

Single NK Cell Activation Assay: NK cells were incubated at 1 million cells per 100 μL in PBA containing IFN- γ Cytokine Catch Reagent and TNF- α Cytokine Catch Reagent at 4 °C for 20 min. Cells were then washed and resuspended in RPMI culture medium supplemented with 2% HS and 1% PS, at 2 million cells mL^{-1} for single-cell encapsulation. Next, the NK cells were encapsulated in 70 pL ($\approx 50 \mu\text{m}$) droplets together with the stimulus (final concentration of K562 cells, 15 million cells mL^{-1} or IL2, 700 ng mL^{-1} or K562+IL2, earlier mentioned concentrations) loaded from another inlet. The concentrations of stimulus have been adjusted such that every single cell received the same absolute number of molecules as in bulk-based experiments. Droplet production and encapsulation rates were carefully monitored using a microscope (Nikon) at 10x magnification and a high-speed camera. The droplet emulsion was collected and covered with a culture medium to protect droplets from evaporation. The encapsulated cells were incubated in Eppendorf tubes with a few punched holes to allow gas exchange, at 5% CO_2 and 37 °C temperature. After 4 h of incubation, the droplets were de-emulsified by adding 20 v/v% PFO (Sigma-Aldrich, 370 533; 100 μL) in HFE-7500 and stained for FACS analysis.

FACS-Antibody Staining: Cells were washed once with PBS and dead cells were stained with Zombie Green fixable viability dye (Biolegend, 423 111, 1:10.000 in PBS, 50 μL) at 4 °C for 20 min. Subsequently, cells were washed once with PBS and incubated with antihuman antibodies against CD3 (PerCP-Cy5.5, Biolegend), CD56 (BV510, Biolegend), CD16 (BV605, Biolegend), CD11b (PE-Cy5, Biolegend) CD27 (AF700, Biolegend) NKp46 (PE, Biolegend), NKg2A (PE-Dazzle 594, Biolegend), IFN- γ (FITC, Miltenyi), and TNF- α (APC, Miltenyi) at 4 °C for 30 min. Next, the cells were washed twice with PBS buffer with 0.5% BSA and analyzed via BD FACS ARIAL.

Single NK Cell Cytotoxicity Assay: NK cells and target cells were labeled with Calcein red (ATT Bioquest; 5 μM) and Cell tracker blue, CMAC (Invitrogen; 10 μM), respectively. The labeled NK cells and target cells were then loaded into droplet chips via different inlets at the concentration of 7 and 10 million cells mL^{-1} , respectively. The viability dyes Sytox Green (Invitrogen) and Cell Event Caspase-3/7 Green (Invitrogen) were loaded at the final concentration of 5 and 7 μM , respectively, along with the cells, and droplets were collected in the observation chamber. Droplets were generated at room temperature, while collected into the observation chamber over a warm water bath. The immobilized droplets were incubated in a stage top incubator set at 5% CO_2 and 37 °C. Image acquisition was performed at every hour interval for 10 h.

Bulk NK Cell Cytotoxicity and Serial Killing Assay: Target cells were labeled with Cell tracker Blue, (CMAC; 10 μM ; Invitrogen) for 30 min at 37 °C and washed after 30 min. PB or HPC-NK cells were cocultured with labeled target cells at different E:T ratio (1:0; 0:1; 1:1; 1:2; 1:3; 2:1;3:1) in a 96-well plate in presence of IL2 (50 ng mL^{-1}). In total, 50 000 cells were maintained in an individual well at a volume of 100 μL . After 8–10 h of incubation, the target cell death was analyzed with FACS using 7AAD viability dye (2 μL per 100 μL cell solution; Stemcell).

Nanoparticle Functionalization: Paramagnetic nanoparticles (Bio-Adebeads Streptavidin Plus 300 nm, Ademtech; 50 μL) were washed with PBS (Gibco; 50 μL) using a magnet. The supernatant was removed, and the nanoparticles were resuspended in PBS (990 μL) with biotinylated anti-IFN- γ (Biolegend) antibodies and incubated for 30 min at room temperature while mixing. Biotin (10 μL) was added with a final concentration of 1 mM in the solution and incubated for 10 min at room temperature. The beads were washed again with PBS using magnets and resuspended in 5% Pluronic F-68 (Gibco) PBS solution and incubated for 30 min at room temperature. The beads were washed and resuspended in assay buffer containing RPMI 1640 (Gibco, life technologies), 5% Human Serum (HS) (Sanquin), and HEPES (Gibco; 25 mM) and incubated for 10 min at room temperature. The nanoparticles were washed again and finally resuspended in the of assay buffer (100 μL) containing fluorescently labeled AlexaFlora568-detection antibody for IFN- γ (Biolegend).

When performing time-lapse experiments with cells, the final nanoparticle suspension contained IL-2 stimuli (Peprotech; 700 ng mL^{-1}) and Sytox Green (Invitrogen; 10 μM) as a final concentration in droplets. For experiments concerning the calibration curve and optimization steps, IFN- γ (Peprotech) cytokine samples ranging from 0.001 to 100 nM were prepared in assay buffer. All calculations were made considering the final concentration inside the droplets.

Image Acquisition and Analysis: Fluorescence imaging was performed using a Nikon Eclipse Ti2 microscope, using a 10X objective and mCherry, DAPI, and FITC/YFP filters every hour. The images were viewed using NIS Element and Image J. Automated Image analysis was performed using custom-made in-build MATLAB script (Mathworks), DMALAB (available with submission). The script generated a droplet mask that was overlaid onto the fluorescence images, and each droplet was analyzed separately. Over 80 000 droplets were analyzed using this script. The output received is in terms of droplet index, cell count, fluorescence intensity, and dead cell count. A detailed description of the image analysis script is provided in Subedi et al.^[24] For the experiments with serial killers, microscopy images were analyzed manually.

Statistics and Software: The graphs were generated using GraphPad Prism 9.0.0. The results are expressed as mean \pm SEM. “n” represents biological repeats with different donors. No technical repeats were performed given the platform only allows a single experiment under given conditions. Significant differences between the two groups were analyzed by a two-way ANOVA followed by Tukey’s multiple comparison test. *p* values < 0.05 were considered statistically significant. Flow cytometry data were analyzed using FlowJo X (Tree Star). Fluorescence Minus One staining served as a control for the gating strategy. For the gating strategy, the readers are referred to Figure S1A (Supporting Information).

Supporting Information

Supporting Information is available from the Wiley Online Library or from the author.

Acknowledgements

These results are part of the project that has received funding from the European Research Council (ERC) under the European Union’s Horizon 2020 research and innovation programme (Grant Agreement No. 802791). Furthermore, the authors acknowledge the generous support from the Eindhoven University of Technology.

Conflict of Interest

The authors declare no conflict of interest.

Author Contributions

N.S., L.V.V., and J.T. designed the study. N.S., L.V.V., and V.K. performed the experiments. K.E. and N.S. developed the observation chambers. M.V.T. and K.E. wrote the script. N.S., L.V.V., L.V.E., and V.K. analyzed the data. N.S., L.V.E., and J.T. wrote the article. P.J., H.D., K.E., and J.B. verified the findings and provided resources for the project. J.T. supervised the research, verified the findings, validated the manuscript, and acquired the funding.

Data Availability Statement

The data that support the findings of this study are available from the corresponding author upon reasonable request.

Keywords

droplet-based microfluidics, effector functions, functional heterogeneity, natural killer cells, NK cell-based immunotherapy, single cell studies

Received: July 21, 2022

Revised: November 25, 2022

Published online: December 14, 2022

- [1] B. Vanherberghen, P. E. Olofsson, E. Forslund, M. Sternberg-Simon, M. A. Khorshidi, S. Pacouret, K. Guldevall, M. Enqvist, K. J. Malmberg, R. Mehr, B. Önfelt, *Blood* **2013**, 121, 1326.
- [2] E. Vivier, E. Tomasello, M. Baratin, T. Walzer, S. Ugolini, *Nat. Immunol.* **2008**, 9, 503.
- [3] C. Shembrey, N. D. Huntington, F. Hollande, *Cancers* **2019**, 11, 1217.
- [4] S. Liu, V. Galat, Y. K. A. Lee, D. Wainwright, J. Wu, *J. Hematol. Oncol.* **2021**, 14, 7.
- [5] W. Hu, G. Wang, D. Huang, M. Sui, Y. Xu, *Front. Immunol.* **2019**, 10, 1205.
- [6] C. Yang, J. R. Siebert, R. Burns, Z. J. Gerbec, B. Bonacci, A. Rymaszewski, M. Rau, M. J. Riese, S. Rao, K. S. Carlson, J. M. Routes, J. W. Verbsky, M. S. Thakar, S. Malarkannan, *Nat. Commun.* **2019**, 10, 3931.
- [7] J. R. Ortaldo, R. B. Herberman, *Annu. Rev. Immunol.* **1984**, 2, 359.
- [8] S. L. Smith, P. R. Kennedy, K. B. Stacey, J. D. Worboys, A. Yarwood, S. Seo, E. H. Solloa, B. Mistretta, S. S. Chatterjee, P. Gunaratne, K. Allette, Y. C. Wang, M. L. Smith, R. Sebra, E. M. Mace, A. Horowitz, W. Thomson, P. Martin, S. Eyre, D. M. Davis, *Blood Adv.* **2020**, 4, 1388.
- [9] A. Ben-Shmuel, G. Biber, M. Barda-Saad, *Front. Immunol.* **2020**, 11, 275.
- [10] N. Subedi, L. P. Verhagen, E. M. Bosman, I. van Roessel, J. Tel, *Cell Immunol.* **2022**, 373, 104497.
- [11] A. Horowitz, D. M. Strauss-Albee, M. Leipold, J. Kubo, N. Nemat-Gorgani, O. C. Dogan, C. L. Dekker, S. Mackey, H. Maecker, G. E. Swan, M. M. Davis, P. J. Norman, L. A. Guethlein, M. Desai, P. Parham, C. A. Blish, *Sci. Transl. Med.* **2013**, 5, 208ra145.
- [12] J. Zhao, S. Zhang, Y. Liu, X. He, M. Qu, G. Xu, H. Wang, M. Huang, J. Pan, Z. Liu, Z. Li, L. Liu, Z. Zhang, *Cell Discovery* **2020**, 6, 22.
- [13] A. Crinier, P. Y. Dumas, B. Escalière, C. Piperoglou, L. Gil, A. Villacreces, F. Vély, Z. Ivanovic, P. Milpied, É. Narni-Mancinelli, É. Vivier, *Cell. Mol. Immunol.* **2021**, 18, 1290.
- [14] M. Efreanova, R. Vento-Tormo, J. E. Park, S. A. Teichmann, K. R. James, *Annu. Rev. Immunol.* **2020**, 38, 727.
- [15] F. Ginhoux, A. Yalin, C. A. Dutertre, I. Amit, *Immunity* **2022**, 55, 393.
- [16] M. Junkin, S. Tay, *Lab Chip* **2014**, 14, 1246.
- [17] N. Sinha, N. Subedi, J. Tel, *Front. Immunol.* **2018**, 9, 2373.
- [18] L. C. Van Eyndhoven, E. Chouri, N. Subedi, J. Tel, *Front. Immunol.* **2021**, 12, 672729.
- [19] F. Wimmers, N. Subedi, N. van Buuringen, D. Heister, J. Vivié, I. Beeren-Reinieren, R. Woestenenk, H. Dolstra, A. Piruska, J. F. M. Jacobs, A. van Oudenaarden, C. G. Figdor, W. T. S. Huck, I. J. M. de Vries, J. Tel, *Nat. Commun.* **2018**, 9, 3317.
- [20] N. Sinha, N. Subedi, F. Wimmers, M. Soennichsen, J. Tel, *J. Vis. Exp.* **2019**, 144, 57848.
- [21] A. M. Abel, C. Yang, M. S. Thakar, S. Malarkannan, *Front. Immunol.* **2018**, 9, 1869.
- [22] I. S. Schuster, J. D. Coudert, C. E. Andoniou, M. A. Degli-Esposti, *Front. Immunol.* **2016**, 7, 235.
- [23] S. Saito, A. Nakashima, S. Myojo-Higuma, A. Shiozaki, *J. Reprod. Immunol.* **2008**, 77, 14.
- [24] N. Subedi, L. C. Van Eyndhoven, A. M. Hokke, L. Houben, M. C. Van Turnhout, C. V. C. Bouten, K. Eyer, J. Tel, *Sci. Rep.* **2021**, 11, 17084.
- [25] I. Prager, C. Liesche, H. Van Ooijen, D. Urlaub, Q. Verron, N. Sandström, F. Fasbender, M. Claus, R. Eils, J. Beaudouin, B. Önfelt, C. Watzl, *J. Exp. Med.* **2019**, 216, 2113.
- [26] S. Antona, I. Platzman, J. P. Spatz, *ACS Omega* **2020**, 5, 24674.
- [27] H. Fujisaki, H. Kakuda, N. Shimasaki, C. Imai, J. Ma, T. Lockey, P. Eldridge, W. H. Leung, D. Campana, *Cancer Res.* **2009**, 69, 4010.
- [28] M. W. H. Roeven, S. Thordardottir, A. Kohela, F. Maas, F. Preijers, J. H. Jansen, N. M. Blijlevens, J. Cany, N. Schaap, H. Dolstra, *Stem Cells Dev.* **2015**, 24, 2886.
- [29] J. S. Hoogstad-van Evert, J. Cany, D. van den Brand, M. Oudenampsen, R. Brock, R. Torensma, R. L. Bekkers, J. H. Jansen, L. F. Massuger, H. Dolstra, *Oncoimmunology* **2017**, 6, e1320630.
- [30] E. Liu, D. Marin, P. Banerjee, H. A. Macapinlac, P. Thompson, R. Basar, L. Nassif Kerbaui, B. Overman, P. Thall, M. Kaplan, V. Nandivada, I. Kaur, A. Nunez Cortes, K. Cao, M. Daher, C. Hosing, E. N. Cohen, P. Kebriaei, R. Mehta, S. Neelapu, Y. Nieto, M. Wang, W. Wierda, M. Keating, R. Champlin, E. J. Shpall, K. Rezvani, *N. Engl. J. Med.* **2020**, 382, 545.
- [31] M. Luevano, A. Madrigal, A. Saudemont, *Cell. Mol. Immunol.* **2012**, 9, 310.
- [32] J. M. R. Van der Meer, R. J. A. Maas, K. Guldevall, K. Klarenaar, P. K. J. D. de Jonge, J. S. H. van Evert, A. B. van der Waart, J. Cany, J. T. Saftir, J. H. Lee, E. Wagena, P. Friedl, B. Önfelt, L. F. Massuger, N. P. M. Schaap, J. H. Jansen, W. Hobo, H. Dolstra, *Cancer Immunol. Immunother.* **2021**, 70, 3367.
- [33] S. Antona, T. Abele, K. Jahnke, Y. Dreher, K. Göpfrich, I. Platzman, J. P. Spatz, *Adv. Funct. Mater.* **2020**, 30, 2003479.
- [34] K. Eyer, R. C. L. Doineau, C. E. Castrillon, L. Briseño-Roa, V. Menrath, G. Mottet, P. England, A. Godina, E. Brient-Litzler, C. Nizak, A. Jensen, A. D. Griffiths, J. Bibette, P. Bruhns, J. Baudry, *Nat. Biotechnol.* **2017**, 35, 977.
- [35] Y. Bounab, K. Eyer, S. Dixneuf, M. Rybczynska, C. Chauvel, M. Mistretta, T. Tran, N. Aymerich, G. Chenon, J. F. Llitjos, F. Venet, G. Monneret, I. A. Gillespie, P. Cortez, V. Moucadel, A. Pachot, A. Troesch, P. Leissner, J. Textoris, J. Bibette, C. Guyard, J. Baudry, A. D. Griffiths, C. Védrine, *Nat. Protoc.* **2020**, 15, 2920.
- [36] Y. J. Yamanaka, C. T. Berger, M. Sips, P. C. Cheney, G. Alter, J. C. Love, *Integr. Biol.* **2012**, 4, 1175.
- [37] R. Bhat, C. Watzl, *PLoS One* **2007**, 2, e326.
- [38] A. E. Christakou, M. Ohlin, B. Vanherberghen, M. A. Khorshidi, N. Kadri, T. Frisk, M. Wiklund, B. Önfelt, *Integr. Biol.* **2013**, 5, 712.
- [39] K. Guldevall, L. Brandt, E. Forslund, K. Olofsson, T. W. Frisk, P. E. Olofsson, K. Gustafsson, O. Manneberg, B. Vanherberghen, H. Brismar, K. Kärre, M. Uhlin, B. Önfelt, *Front. Immunol.* **2016**, 7, 119.

- [40] S. Sarkar, P. Sabhachandani, D. Ravi, S. Potdar, S. Purvey, A. Beheshti, A. M. Evens, T. Konry, *Front. Immunol.* **2017**, *8*, 1736.
- [41] X. An, V. G. Sendra, I. Liadi, B. Ramesh, G. Romain, C. Haymaker, M. Martinez-Paniagua, Y. Lu, L. G. Radvanyi, B. Roysam, N. Varadarajan, *PLoS One* **2017**, *12*, e0181904.
- [42] A. Müllbacher, K. NJ, *John Curtin School of Medical Research, Australian National University, Canberra, Australia.*
- [43] J. D. Fayen, M. L. Tykocinski, *Immunology* **1999**, *97*, 272.
- [44] R. Ramirez, R. Solana, J. Carracedo, M. C. Alonso, J. Peña, *Cell. Immunol.* **1992**, *140*, 248.
- [45] S. Tsuchiya, M. Yamabe, Y. Yamaguchi, Y. Kobayashi, T. Konno, K. Tada, *Int. J. Cancer* **1980**, *26*, 171.
- [46] C. Lehmann, M. Zeis, L. Uharek, *Br. J. Haematol.* **2001**, *114*, 660.
- [47] R. Wang, J. J. Jaw, N. C. Stutzman, Z. Zou, P. D. Sun, *J. Leukoc Biol.* **2012**, *91*, 299.
- [48] A. Chauveau, A. Aucher, P. Eissmann, E. Vivier, D. M. Davis, *Proc. Natl. Acad. Sci. USA* **2010**, *107*, 5545.
- [49] T. Kataoka, N. Shinohara, H. Takayama, K. Takaku, S. Kondo, S. Yonehara, K. Nagai, *J. Immunol.* **1996**, *156*, 3678.